Revealing the Dimeric Crystal and Solution Structure of -Lactoglobulin at pH 4 and Its pH and Salt Dependent Monomer–Dimer Equilibrium

Khan, Sanaullah; Ipsen, Richard; Almdal, Kristoffer; Svensson, Birte; Harris, Pernille

Published in:
Biomacromolecules

Link to article, DOI:
10.1021/acs.biomac.8b00471

Publication date:
2018

Document Version
Peer reviewed version

Revealing the dimeric crystal and solution structure of β-lactoglobulin at pH 4 and its pH and salt dependent monomer-dimer equilibrium

Sanaullah Khan[†, §,], Richard Ipsen[‡], Kristoffer Almdal[§], Birte Svensson[†] and Pernille Harris[//,]**

[†]Enzyme and Protein Chemistry, Department of Biotechnology and Biomedicine, Technical University of Denmark, Søltofts Plads, Building 224, DK-2800 Kgs. Lyngby, Denmark

[§]Department of Micro- and Nanotechnology, Technical University of Denmark, Ørsteds Plads, Building 423, DK-2800 Kgs. Lyngby, Denmark

[‡]Department of Food Science, University of Copenhagen, Rolighedsvej 26, DK-1958 Frederiksberg, Denmark

[//]Department of Chemistry, Technical University of Denmark, Kemitorvet, Building 207, DK-2800 Kgs. Lyngby, Denmark

ABSTRACT

The dimeric structure of bovine *β*-lactoglobulin A (BLGA) at pH 4.0 was solved to 2.0 Å resolution. Fitting the BLGA pH 4.0 structure to SAXS data at low ionic strength (goodness of fit *R*-factor = 3.6%) verified the dimeric state in solution. Analysis of the monomer-dimer equilibrium at varying pH and ionic strength by SAXS and scattering modeling showed that BLGA is dimeric at pH 3.0 and 4.0, shifting towards a monomer at pH 2.2, 2.6 and 7.0 yielding monomer/dimer ratios of 80/20%, 50/50% and 25/75%, respectively. BLGA remained a dimer at pH 3.0 and 4.0 in 50–150 mM NaCl, whereas the electrostatic shielding raised the dimer content at pH 2.2, 2.6 and 7.0, i.e. below and above the pI. Overall the findings provide new insights on the molecular characteristics of BLGA relevant for dairy product formulations and for various biotechnological and pharmaceutical applications.

***Keywords*:** β-lactoglobulin A; X-ray crystallography; small-angle X-ray scattering; scattering modeling; monomer/dimer ratios

INTRODUCTION

β-Lactoglobulin (BLG) is a small soluble and acid stable globular protein with molecular mass of ~18.4 kDa (162 amino acid residues) and isoelectric point of 4.7–5.2,[1,2,3] found in bovine milk at 3.0–3.3 g/L.[4,5] It occurs in several isoforms of which two, BLGA and BLGB, are dominant.[6] BLGA is most common and differs at Gly64 and Val118 being Asp64 and Ala118 in BLGB.[7, 8] BLG is a member of the lipocalin family able to bind and transport small, typically hydrophobic molecules like retinol, fatty acids, vitamins and dodecyl sulphate.[9–14] While the biological function of BLG remains unknown, it has been suggested to serve a role in nutrition and as carrier of small ligands.[9–15] Notably, BLG is highly relevant with applications in the food, biotechnology and pharmaceutical industries.[9,10,14,15]

Crystal and NMR structures revealed that BLG has a hydrophobic core of eight antiparallel β-strands (A-H) forming a β-barrel (or calyx) showing a pH dependent accessibility mediated via a conformational change of the flexible loop connecting strands E and F (EF-loop-residues 85–90).[10,16] At pH >7.0 this loop adopts an open conformation as seen in different crystal structures (1BEB, 1BSY, 1B0O, 2Q2M, 2BLG),[1,14,17–19] whereas at pH <7.0 a closed form is found in crystal and NMR structures (1CJ5, 2AKQ and 3BLG).[19, 20, 21]

In solution BLG is present in different oligomerization states depending on pH, ionic strength and temperature.[6,22,23] Previous studies have shown that BLGA is a monomer at pH ≤ 3,[6,24–27] a dimer at neutral pH[6,15,23] and exists as a dimer-octamer equilibrium at pH 4.7 depending on ionic strength.[6] NMR structures of BLGA monomers were determined at pH 2.0 (in 20 mM HCl, 5 mg/mL BLGA, 45°C)[20] and pH 2.6 (in 50 mM potassium phosphate, ~20 mg/mL BLGA, 37°C)[27] opposed to crystal structures at pH 5.2–8.2, where BLGA is a dimer at different ionic strengths.[1,14,17,19,21,28,29] Previous proton magnetic relaxation dispersion (MRD) and light scattering studies have shown that BLGA forms larger structures, i.e. tetramers, hexamers and octamers at pH 3.7–5.0 at 15°C and below 10°C.[6,

[30–32] BLGA associates to form these large structures at high protein concentrations (>15 mg/mL), and this association increases with increase in protein concentration and decrease in temperature.[32,33] BLGA (at <10 mg/mL) exists as a monomer-dimer equilibrium at pH <4.0 and >5.2 and the equilibrium shifts towards the dimer with increasing ionic strength and decreasing charge on the protein,[33] and towards the monomer with increase in temperature.[27] Sedimentation velocity analysis provided evidence that BLGA is a dimer with no larger oligomer being present at pH 4.5 and 5.5 in 20 mM sodium citrate/citric acid, 100 mM NaCl at 25°C.[34]

Although BLG has been extensively investigated, the tertiary structure at pH 4.0 has not been reported. This pH region, however, is highly relevant e.g. for food applications such as acidified milk drinks and many protein enriched food products, which motivated the present structure determination of BLGA in the crystal and in solution at pH 4.0. Furthermore, SAXS combined with scattering modelling enabled analysis of BLGA self-association and provided estimates of the shift in monomer/dimer ratio elicited by change of pH and ionic strength.

MATERIALS AND METHODS

Sample preparation. β-lactoglobulin variant A (BLGA) was purified from cow's milk as described previously,[35] and the purity of the sample was verified by analytical ultracentrifugation. Lyophilized BLGA (6 mg/mL) was dissolved in milliQ water by stirring (150 rpm, overnight, R.T.), centrifuged (12,000 *g*, 20 min, 4°C) and filtered (0.22 μm syringe filter; Frisenette ApS, Knebel, Denmark). The BLGA concentration was determined spectrophotometrically at 280 nm using a molar extinction coefficient ε = 17,600 $M^{-1} \cdot cm^{-1}$. [35] The BLGA stock solution was diluted buffers to 10 mM glycine (pH 2.2 and 2.6), sodium citrate/citric acid (pH 3.0 and 4.0), and Tris-HCl (pH 7.0). The sample was equilibrated for ~2 h by adding fresh buffers using 3 kDa cutoff centrifuge based filters and centrifuged

(12,000 *g*, 20 min, 4°C). BLGA (15 mg/mL) in 50 mM sodium citrate/citric acid pH 4.0 was used for crystallization (see below).

BLGA crystallization. Crystals were grown at pH 4.0 in hanging drops containing 2 µL BLGA (15 mg/mL) and 2 µL 12% PEG 4000, 150 mM magnesium nitrate, for about two weeks at R.T. Prior to data collection, BLGA crystals were cryoprotected in crystallization liquid containing 25% glycerol and flash-frozen in liquid nitrogen. Data were collected from a rod-shaped crystal at the ESRF (Grenoble, France) on beamline ID30A-1 (MASSIF-1) using a Pilatus3 2M detector. The size of the crystal was about 0.6 mm in length and 0.15 mm in width. The data were processed and scaled using the programs XDS and XSCALE.[37] Data collection and data processing statistics are summarized in Table 1.

Structure determination and refinement. The BLGA structure was solved by molecular replacement in Phaser,[38] using the crystal structure of BLGA determined at pH 7.3 (1BSO) as search model.[19] An initial model was obtained using AutoBuild,[39] and improved by several cycles of refinement, manual building and water picking using WinCoot[40] and PHENIX.[41,42] Refinement statistics are summarized in Table 1.

SAXS of BLGA. SAXS experiments of BLGA in the absence and presence of salt at various pH were performed on beamline BM29 (ESRF, Grenoble, France)[43] and beamline P12 (EMBL, DESY, Hamburg, Germany).[44] Samples were measured at 20°C in 10 time frames with exposure times of 2 s (ESRF) and 0.05 s (DESY) each. The exposure time was optimized using on-line checks during acquisitions to avoid radiation damage effects. All frames were averaged in order to maximize signal-to-noise ratios for each data-set after visual inspection. The sample-to-detector distance was 2.867 m (ESRF) and 3.0 m (DESY). Sample size was approximately 40 µL using an automated flow cell. Buffers were measured before and after each sample and averaged prior to subtraction. Buffer

averaging and subtraction prior to data analysis was done in PRIMUS.[45] Data were collected for 1 mg/mL BLGA in 10 mM glycine (pH 2.2 and 2.6), sodium citrate/citric acid (pH 3.0 and 4.0), and Tris-HCl (pH 7.0) in the absence and presence of NaCl. The Guinier analysis was done using PRIMUS[44] and the distance distribution function was calculated using GNOM.[46]

Scattering modeling. The calculations of X-ray scattering curves for BLGA monomer determined at pH 2.0 (1CJ5) and the present dimer crystal structure at pH 4.0 (6FXB) were performed for comparison with the experimental curves using SCT.[47, 48] A cube side length of 0.591 nm and a cutoff of four atoms were used to create spheres in the BLGA models. The hydration shell (0.3 g H_2O/g protein) was created by adding spheres to the unhydrated sphere models using HYPRO.[47, 49] The X-ray scattering curve *I(Q)* was calculated using the Debye equation (adapted to spheres) as described previously.[47,50]

RESULTS AND DISCUSSION

Structure of BLGA. The structure at pH 4.0 was solved by molecular replacement to 2.0 Å resolution (refinement statistics are shown in Table 1). Four BLGA monomers making two well defined dimers (AB and CD) were found in the asymmetric unit. The Ramachandran plot showed all residues to be within allowed regions except Tyr99 that adopts a γ-turn conformation in all four chains, a common feature to nearly all BLGA structures.[14,18,19]

Essentially the overall structure of the BLGA monomers corresponds well to previously reported structures.[14,18–19] The BLGA monomer consists of one main α-helix (residues 130–142) and nine β-strands (A–I), eight (A–H) forming a β-barrel, while β-strand I contributes to the dimer interface (Figure 1A and B). The present structure includes four short α-helices, α-1, α-2, α-3 and α-4 (Figure 1B). All four chains have the EF loop in closed conformation as expected for acidic conditions.[19,21,21]

Table 1. Data Collection and Refinement Statistics for BLGA

Data collection	
Space group	$P22_12_1$
Unit cell	
a, b, c (Å)	67.11, 75.61, 140.62
α, β, γ (º)	α= 90, β=90, γ=90
Total number of reflections	198216(12719)
Number of unique reflection	46190(3397)
Protein molecules in ASU	4
Resolution limits (Å)	60.56–1.99(2.04–1.99)
Rmerge (%)	6.6(52.9)
Completeness (%)	92.5(93.6)
Average I/σ (I)	11.46(2.67)
Wilson plot B-factor ($Å^2$)	29.7
Refinement	
R_{factor} (%)	23.21(30.26)
R_{free} (%)	26.95(35.35)
Number of reflections	45896(4632)
Reflections used for R-free	2267(227)
Number of residues in ASU	648
Number of water molecules	230
Root mean square deviation from ideal	
Bond lengths (Å)	0.005
Bond angles (º)	0.84
B-factors ($Å^2$)	41
Solvent content	49.8
Rotamers and Ramachandran Plot	
Ramachandran outliers (%)	0
Rotamer outliers (%)	0.87
Residues in preferred regions (%)	97
Residues in allowed regions (%)	3

The open and closed conformations of the EF loop are also illustrated in various structures by the distance between C_α-L87 (EF loop) and C_α-P38 (AB loop) (Table S1).

Using PyMOL,[51] the secondary structure elements in the present crystal structure were compared with earlier crystal structures covering the pH range 5.2–8.5; 2AKQ (pH 5.2);[21] 3BLG (pH 6.2);[18] 1BEB (pH 6.5);[1] 1BSQ (pH 7.1);[29] 1BSO (pH 7.3);[19] 2Q2M (pH 7.4);[17] 2BLG (pH 8.2); [18] and 5HTE (pH 8.5)[52] as well as with two NMR structures: 1CJ5 (pH 2.0)[20] and 1DV9 (pH 2.6)[27] (Table S1). Helix α-1 (residues 12–15 in the N-terminal loop) is several residues longer in some of these other BLGA structures and not well conserved in the lipocalin family.[1,19] α-2 (residues 29–33 in the AB loop) in previously reported structures was formed by residues 29–32 and is together with strand I situated at the dimer interface and lacking in the NMR monomer structures determined at pH 2.0 (1CJ5)[18] and at pH 2.6 (1DV9).[27] α-2 may thus be required for stabilization of the dimeric state. α-3 (residues 113–116 in the GH loop) was found in the present pH 4.0 crystal structure and in the crystal structure determined at pH 6.5, but lacking in all other reported crystal [1,17-19,21,52] and NMR structures,[20, 27] and hence is not well conserved (Table S1). α-4 (residues 153–157 in the C-terminal loop) was similar in the present pH 4.0 and crystal structures at pH 5.2 (2AKQ),[21] pH 6.2 (3BLG),[18] and pH 8.2 (2BLG),[18] one residue longer than in structures at pH 2.0 (1CJ5)[20] and 6.5–7.3 (1BSO, 1BSQ, 1BEB),[1,19, 29] one residue shorter than in the NMR structure at pH 2.6 (1DV9)[27] (Table S1), and lacking in the crystal structure at pH 8.5. These observations together indicate that α-4 is not strictly conserved.

The BLGA dimer interface contained five hydrogen bonds; four inter-monomer main chain hydrogen bonds observed in all structures: Arg148:N (A)→Arg148:O (B), Ser150:N (A)→His146:O (B), Arg148:N (B)→Arg148:O (A), Ser150:N (B)→A:His146:O (A) (Figure 1C) between β-strands I in two monomers, and a side-chain hydrogen bond His146:ND1 (A)→Ser150:O (B) only observed in the present pH 4.0 crystal structure (Figure 1C). These inter subunit hydrogen bonds between β-strands I

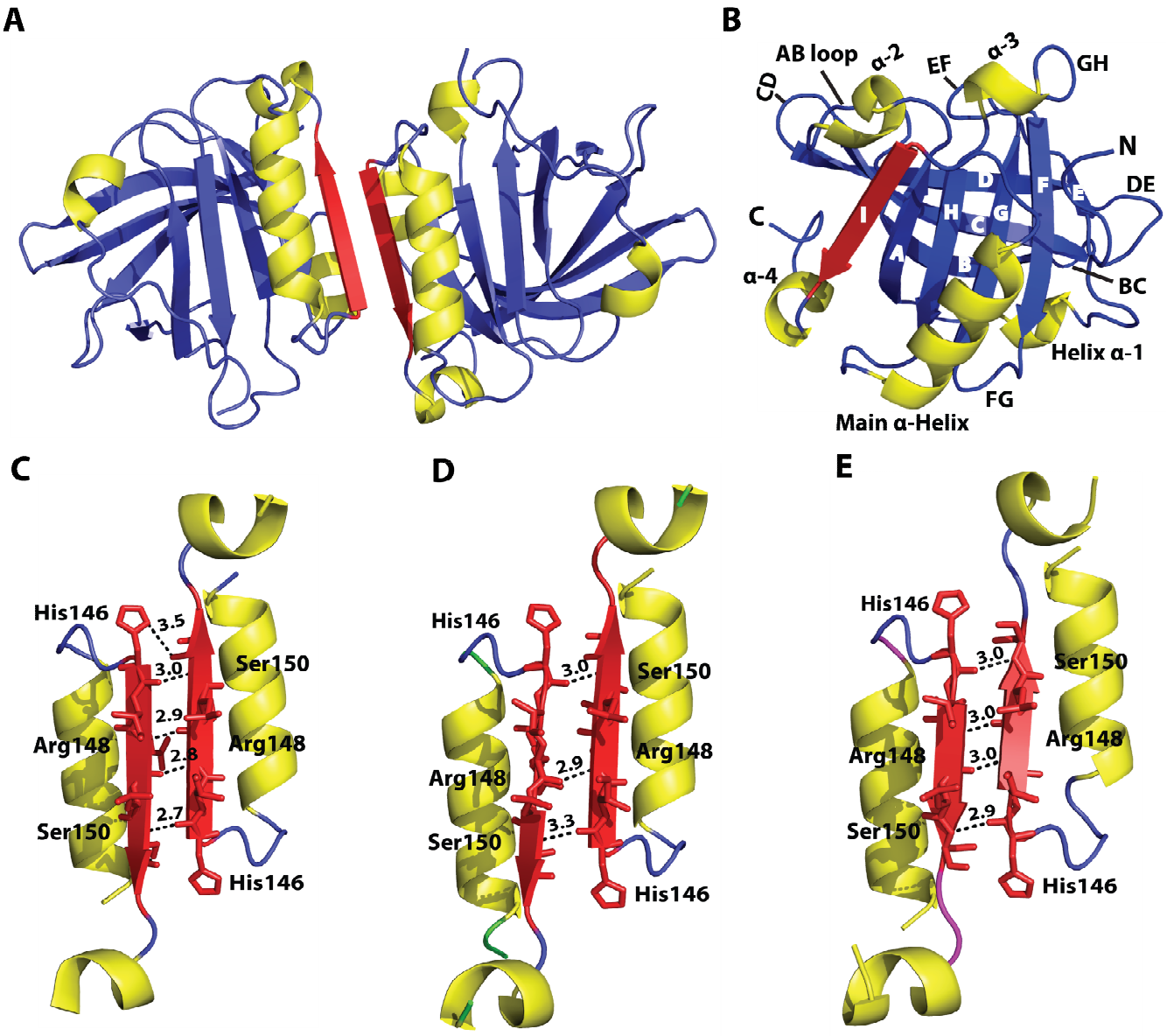

Figure 1. Crystal structure of BLGA (6FXB) at pH 4.0. (A) Ribbon representation of BLGA (chains AB) dimer. (B) Ribbon representation of a BLGA (chain B) monomer with β-strands, α-helices and loops being labeled. The dimer interface of BLGA (chains AB) showing hydrogen bonds between β-strands I in (C) the present crystal structure at pH 4.0, and crystal structures (D) at pH 5.2 (2AKQ) and (E) pH 6.5 (1BEB). This figure was generated by PyMOL.[51] Hydrogen bond distances are shown in angstrom (Å).

are critical for dimer stability. The number of inter subunit hydrogen bonds between β-strands I in the present structure were compared with other reported structures and are shown in Table S1, Figure 1C,D

and E. It is important to mention that the missing hydrogen bonds in some structures could also be due to low resolution.

Superimposition of the BLGA (chains AB) dimer with dimeric crystal structures (1BEB, rmsd 1.2Å) showed the structures varied from each other mostly in flexible loops and helices (Figure 2A). Superimposition of the BLGA monomer (chain B) at pH 4.0 with monomeric BGLA determined by NMR at pH 2.0 (1CJ5)[20] and 2.6 (1DV9),[27] showed striking conformational differences involving the AB loop that occur at the dimer interface in the main α-helix (Figure 2B). The conformations of Phe105 and Met107 inside the calyx, and Trp19 at the base of calyx were different from the NMR structures at pH 2.0 (1CJ5: 10 models) and at pH 2.6 (1DV9: 21 models) (Figure 2B, Figure S1). The presence of these differences for the BLGA monomer subunit was evident also from the rms deviation (C_α) of 1.8–2.1 Å for 1CJ5[20] (10 models) and 0.93–1.30 Å for 1VD9 (21 models).[27] The BLGA structure at pH 4.0 also contained one polyethylene glycol and two nitrate ions that came from the crystallization solution.

SAXS of BLGA. Self-association of BLGA as a function of pH and ionic strength was studied using SAXS at the beamline BM29 ESRF (Grenoble, France).[43] The scattering data for BLGA showed no radiation damage. The Guinier fits of BLGA (1 mg/mL) gave R_G values of 1.73 ± 0.02 nm (pH 2.2), 1.94 ± 0.03 nm (pH 2.6), 2.39 ± 0.03 nm (pH 3.0), 2.32 ± 0.04 nm (pH 4.0) and 2.09 ± 0.02 nm (pH 7.0) (Table S2). At 2 mg/mL, the R_G values increased slightly to 1.80 ± 0.02 nm (pH 2.2), 2.01 ± 0.03 nm (pH 2.6) and 2.2 ± 0.02 nm (pH 7.0). However, at pH 3.0 and 4.0 the R_G values were similar to the values observed for BLGA at 1 mg/mL (Table S3, Figure 3), indicating concentration dependent self-association of BLGA at pH 2.2, 2.6 and 7.0. The results from the Guinier analyses agreed very well

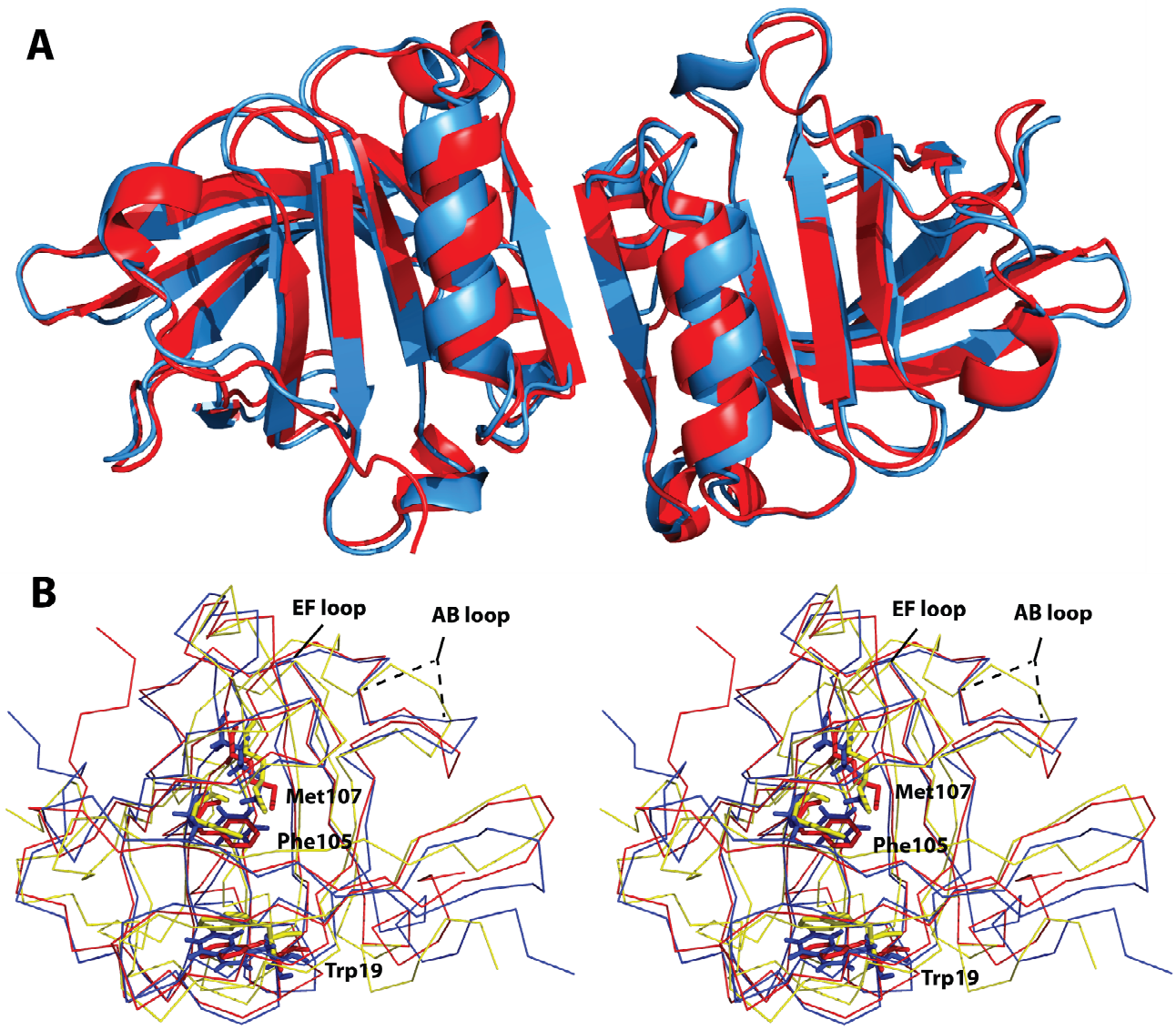

Figure 2. (A) Superimposition of BGLA dimer at pH.4.0 (red, 6FXB) and the crystal structure of BLGA at pH 6.5 (sky blue, 1BEB). (B) Stereo view showing BLGA structural comparisons. Superimposition of the present BGLA (chain B) single subunit at pH 4.0 (red) and the monomer NMR structures of BLGA at pH 2.0 (yellow, 1CJ5, first model), and at pH 2.65 (blue, 1DV9, first model).

with the corresponding R_G and maximum length L values calculated using GNOM[46] (Table S2, Table S3, Figure 3, Figure S3, Figure S4). These R_G and L values were compared to an R_G of 1.59

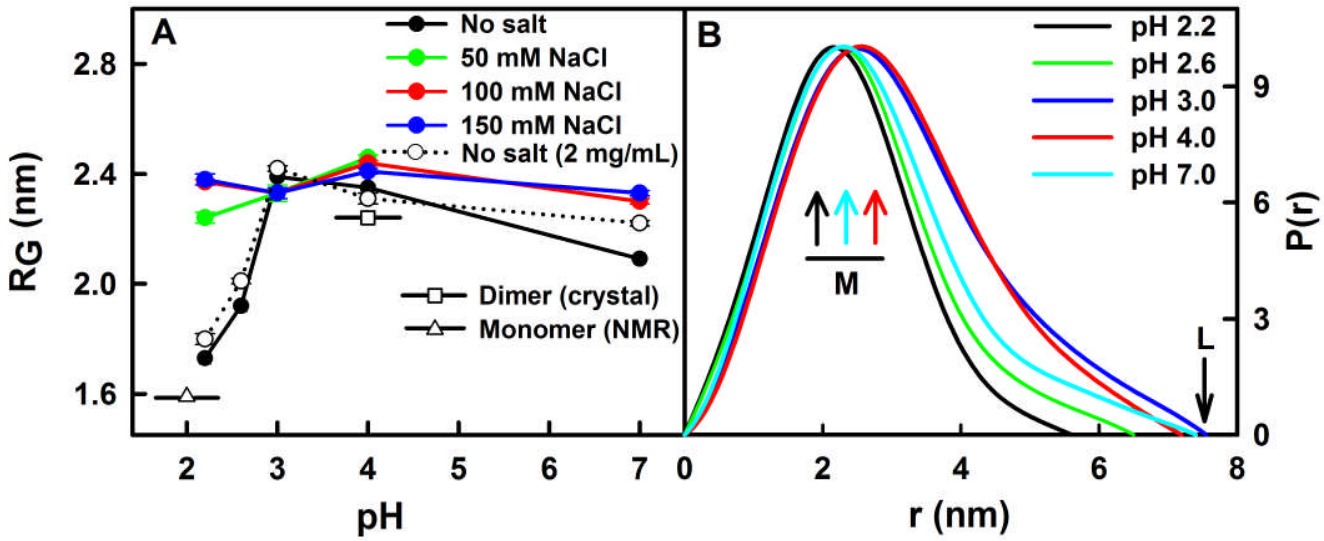

Figure 3. Experimental Guinier and *P*(*r*) analyses of BLGA. BLGA at 1 mg/mL in the presence and absence of NaCl and at 2 mg/mL (0 M NaCl) was analysed in 10 mM glycine (pH 2.2 and 2.6), sodium citrate/citric acid (pH 3.0 and 4.0) and Tris-HCl (pH 7.0). (A) Guinier R_G values for BLGA. The theoretical R_G values calculated for the dimeric pH 4.0 crystal structure determined in the present work (open square) and monomer NMR structure (open triangle) are shown for comparison. (B) Distance distribution function *P*(*r*) analyses of BLGA at various pH. The most frequently occurring distance *M* and the maximum length *L* for BLGA are indicated. The *L* was measured when the *P*(*r*) curve reached zero at a large *r* value.

nm and *L* of 4.5 nm calculated for the monomeric NMR structure (1CJ5)[20], and an R_G of 2.26 nm and *L* of 7.1 nm calculated for the present dimeric crystal structure (Figure 3) and to R_G values reported for BLGA in the literature.[23,33] The results indicated that the solution state behavior of BLGA as a function of pH can be categorized as: i) pH<3.0, the R_G of BLGA was lower than the R_G value observed for the dimer and higher than for the monomer, indicating a mixed population of monomer and dimer; ii) pH 3.0 and 4.0, the R_G was in similar range as observed for the dimer, suggesting that BLGA exists as a dimer at pH 3.0 and 4.0, iii) pH 7.0, the R_G was lower than the dimer, and higher than observed for the monomer, indicating a mixed population of monomer and

dimer, and iv) an increase in BLGA concentration increased the dimer proportion at pH 2.2, 2.6 and 7.0, indicating concentration dependent self-association of BLGA at these pH values. In conclusion BLGA exists as dimer at pH 3.0 and 4.0 and as a monomer-dimer equilibrium outside this pH range.

Scattering modeling. A more thorough investigation of the monomer-dimer equilibrium was performed by fitting analysis of the experimental scattering curves to the theoretically calculated curves of the BLGA monomeric NMR structure (1CJ5)[20], the pH 4.0 dimeric crystal structure, and their merged scattering curves using different weights for comparison with experimental data using SCT, a software suite for comparing atomistic models with SAXS data.[47, 48] The monomer and dimer curves were merged for complementary weights of 0–80%/100–20%, and fitted to the experimental data to estimate the percent proportion of monomer and dimer. Fitting analyses of merged theoretical curves of monomer and dimer to experimental data (1 mg/mL) resulted in excellent fits using weights of 80/20% for pH 2.2, 50/50% for pH 2.6 and 25/75% for pH 7.0 (Figure 4A, B, E and F), suggesting that BLGA exist as mixed population of monomer and dimer. The goodness of *R* factor values for merged curves were 2.3, 1.9 and 3.5% for BLGA at pH 2.2, 2.6 and 7.0, respectively. The merged curves gave R_G values of 1.72, 1.91 and 2.06 nm, and maximum length *L* values of 5.5, 6.8 and 7.0 nm at pH 2.2, 2.6 and 7.0, respectively, in excellent accord with the corresponding experimental *L* values of 5.6, 6.5 and 7.4 nm (Figure 4A, B and E insets, Table S2). At 2 mg/mL, weights of 70/30% for pH 2.2, 39/61% for pH 2.6 and 19/81% for pH 7.0 resulted in excellent fits with *R* factor of 3.8%, 3.7% and 2.7%, respectively. The merged curves resulted in R_G values of 1.78, 1.98 and 2.1 nm, in good agreement with experimental data (Table S3). Curve fitting analyses gave good fits with an *R* factor of 4.7% and 5.6% at pH 3.0 and 2.3% and 3.6% at pH 4.0 for BLGA dimer at 1 and 2 mg/mL, respectively. The maximum length *L* of 7.1 nm for BLGA dimer agreed well with the experimental *L* values of 7.1 and

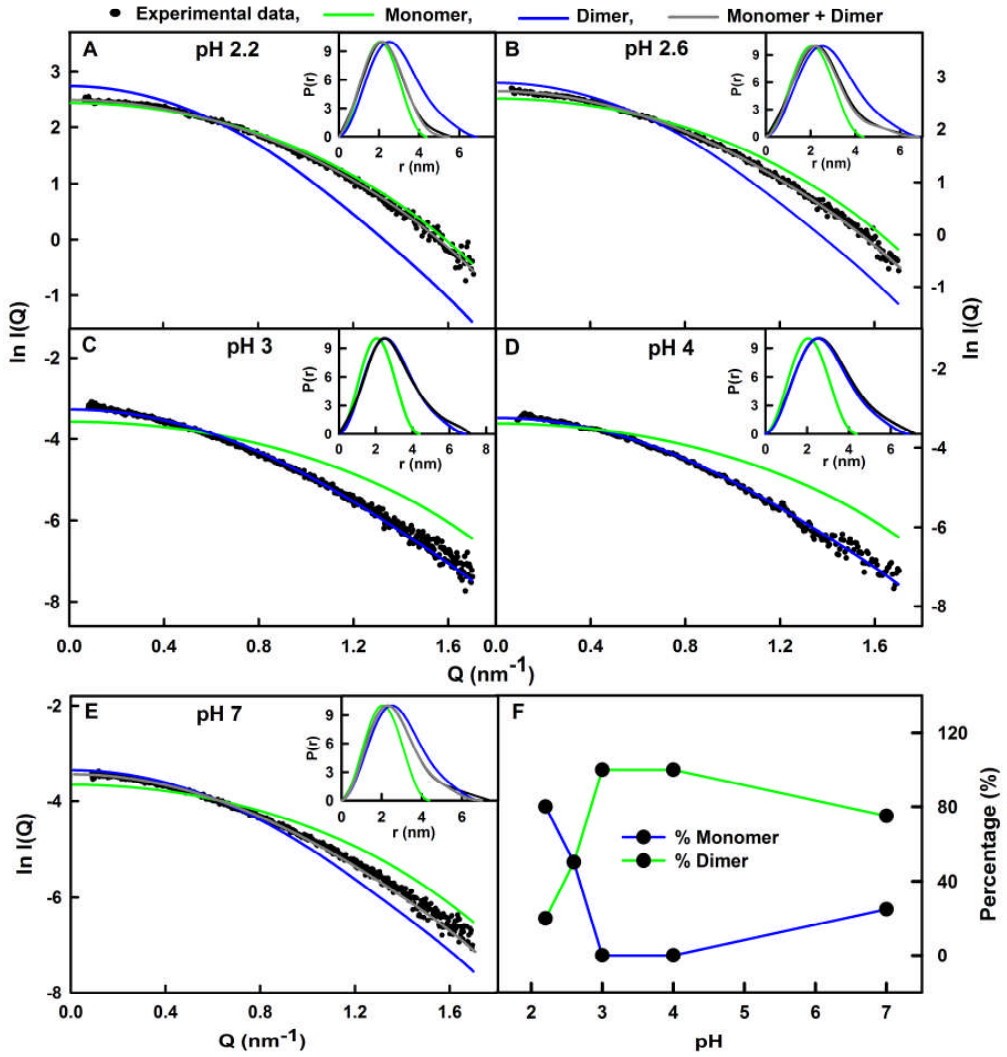

Figure 4. The main panels (A-E) depict the *I*(*Q*) curve fits, and the insets show the *P*(*r*) distance distribution function fits. The experimental *I*(*Q*) and *P*(*r*) scattering data of BLGA (1 mg/mL in 10 mM glycine (pH 2.2 and 2.6), sodium citrate/citric acid (pH 3.0 and 4.0) and Tris-HCl (pH 7.0), 0 M NaCl) are represented by black circles and lines, respectively; the green and blue lines correspond to the pH 2.0 monomeric NMR structure (1CJ5) and the pH 4.0 dimeric crystal structure (6XFB), respectively. The gray lines correspond to the merged curves of monomer and dimer using scattering weights of 80/20% at pH 2.2 (A), 50/50% at pH 2.6 (B), 25/75% at pH 7.0 (E). (F) Percentage of monomer and dimer derived from fitting analyses of monomer, dimer and monomer/dimer merged curves using various scattering weights. The maximum lengths *L* of monomer, dimer and monomer/dimer merged curves are shown for comparisons in the *P*(*r*) curves (insets). The *L* was measured when the *P*(*r*) curve reached zero at a large *r* value.

7.8 nm at pH 3.0 and 7.2 and 7.5 nm at pH 4.0 at 1 mg/mL and 2 mg/mL (Figure 4C and D, Table S2, Table S3), thus validating the crystal and the SAXS data. Converting these ratios of monomer-dimer into percent dissociation resulted in K_D of 345.6 μM for 80/20%, 54 μM for 50/50% and 9 μM for 25/75% monomer-dimer at 1 mg/mL. The K_D value of 345.6 μM observed for BLGA at pH 2.2 was larger than the K_D values of 91 μM reported for BLG prepared from pooled milk ($BLGB^{Prep\ II}$) at pH 2.2[53] in 0.1 M NaCl. At pH 2.6, the K_D value of 54 μM observed for BLGA was larger than the K_D values of 15 μM reported at pH 2.5[34] and was smaller than the K_D value of 130 μM measured at pH 2.7[54]. The K_D value of 9 μM at pH 7.0 observed for BLGA was smaller than the K_D values of 20, 21, 24 μM reported for BLGA at pH 6.9–7.0 at 20°C.[55–57] These results indicated that BLGA exists as monomer-dimer equilibrium in this pH range although their reported values were obtained at 0.1–0.13 M NaCl.[54,34] These differences in K_D values can be attributed to different temperature and ionic strength. An increase in temperature destabilizes the dimeric state,[24] shifting the monomer-dimer transition towards the monomer. The monomeric state of BLGA studied by NMR at 37°C (pH 2.6) and 45°C (pH 2.0) could be a consequence of high temperature compared to the monomer-dimer equilibrium at pH 2.2 and 2.6 at 20°C observed by using SAXS. At pH 3.0 and pH 4.0, our scattering fits analyses showed that BLGA exists as a dimer, contrary to previously reported data at pH 3.0 in 0.1 M NaCl (K_D 63 μM).[24]

Dependence of NaCl. In the presence of 50–150 mM NaCl, R_G values were between 2.24 and 2.41 nm and scattering curves at pH 2.2, 2.6 and 7.0 showed a good fit to the dimeric structure (Table S2, Figure S5). These data suggest that NaCl increased the dimer population by shielding intermolecular electrostatic charge repulsions, hence stabilizing the dimeric state through hydrophobic and specific electrostatic interactions, in agreement with reported data[24,34] No significant changes were observed when NaCl was added to the BLGA solution at pH 3.0 and 4.0 (Table S2, Figure 3A, Figure S3). In

summary, these data suggest that BLGA dimeric structure is stable at pH 3.0 and 4.0, supporting the dimeric crystal structure at pH 4. The stability of the dimeric structure at pH 4.0 could be attributable to the formation of five inter submit hydrogen bonds between two monomer β-strands I.

CONCLUSIONS

By this study, we have determined structure of the BLGA in the crystal and in solution at pH 4.0 and characterized monomer–dimer equilibrium as a function of pH and ionic strength. BLGA differs from other structures in several aspects involving variations in flexible loops and small helices – most notably the AB loop conformation and the two monomer β-strands I forming an intermolecular antiparallel β-sheet that contains five hydrogen bonds, which seem to be required for stabilization of the dimer interface at pH 4.0. By SAXS and scattering modeling, we observed dimer-to-monomer transition at pH <3.0 and at pH 7.0, attributable to intermolecular electrostatic charge repulsion between BLGA monomers. We determined the percent proportion of monomer and dimer over a pH range of 2.2–4.0 and at pH 7.0 and showed that the dimer proportion was increased with increase in concentration of BLGA at pH 2.2, 2.6 and 7.0, indicating concentration dependent self-association of BLGA. Additionally, we investigated the effect of salt on the solution state behavior of BLGA, and found that although salt has no significant effect at pH 3.0 and 4.0, it at pH 2.2, 2.6 and 7.0 shifts the monomer-dimer equilibrium towards the dimer. This increase in the dimer proportion is attributable to counter ions shielding electrostatic charge repulsions and suggests that the dimer is stabilized by intrinsic hydrophobic and specific electrostatic interactions. The findings provide detailed novel information on molecular properties of BLGA of relevance to industrial applications, as i) BLG and its nanocomplexes with polysaccharides have potential as delivery systems for drugs and nutraceuticals,[2,58–66] ii) BLG used as enhancer for poorly absorbed bioactives[58,59] and iii) BLG at pH

4.0 is important for formulation of different food products with other biological macromolecules (e.g. polysaccharides) added as ingredients.

PDB accession number

The coordinates for BLGA been deposited in the Protein Data Bank with accession code 6FXB.

ASSOCIATED CONTENT

Supporting information

Supporting Tables and Figures showing the following: Comparisons of secondary structure elements of BLGA at different pH; Stereo views of BLGA showing structural comparisons; Guinier R_G and $P(r)$ analyses of BLGA at various pH; SAXS data for BLGA (1 mg/mL) at different pH and NaCl concentration; SAXS data for BLGA (2 mg/mL) at different pH values; pH and NaCl concentration dependence of GNOM R_G parameters for BLGA; Experimental $P(r)$ analyses of BLGA; X-ray scattering curve fits for the monomer and dimer BLGA structures.

AUTHOR INFORMATION

Corresponding Author

Enzyme and Protein Chemistry, Department of Biotechnology and Biomedicine, Technical University of Denmark, Søltofts Plads, Building 224, DK-2800 Kgs. Lyngby, Denmark,

phone: +4545252751; Email: sank@dtu.dk (S. Khan)

Department of Chemistry, Technical University of Denmark, Kemitorvet, Building 207, DK-2800 Kgs. Lyngby, Denmark, phone: +4545252024, Email: ph@kemi.dtu.dk (P. Harris)

Acknowledgements

We thank Karina Jansen for valuable technical assistance. This project was funded by the Danish Council for Independent Research | Technical and Production Sciences to the project “HEXPIN.

Associative interactions between exopolysaccharides from lactic acid bacteria and milk proteins. Gaining insights deployable in design and optimised food texture". The ESRF and EMBL Hamburg synchrotrons are thanked for beam time and outstanding support during data collection. The research presented has received funding from BioStruct-X and DANSCATT (the Danish agency for Science, Technology and Innovation).

REFERENCES

(1) Brownlow, S.; Cabral, J. H. M.; Cooper, R.; Flower, D. R.; Yewdall, S. J.; Polikarpov, I.; North, A. C.; Sawyer, L. Bovine β-lactoglobulin at 1.8 Å resolution — still an enigmatic lipocalin. *Structure* **1997**, *5* (4), 481–495.

(2) Hosseini, S. M. H.; Emam-Djomeh, Z.; Sabatino, P.; Van der Meeren, P. Nanocomplexes arising from protein-polysaccharide electrostatic interaction as a promising carrier for nutraceutical compounds. *Food Hydrocoll.* **2015**, *50*, 16–26.

(3) Hosseini, S. M. H.; Emam-Djomeh, Z.; Razavi, S. H.; Moosavi-Movahedi, A. A.; Saboury, A. A.; Atri, M. S.; Van der Meeren, P. β-Lactoglobulin-sodium alginate interaction as affected by polysaccharide depolymerization using high intensity ultrasound. *Food Hydrocoll.* **2013**, *32* (2), 235–244.

(4) Bell, K.; McKenzie, H. A. Beta-lactoglobulin. *Nature* 1964, *204*, 1275–1279.

(5) Konrad, G.; Lieske, B.; Faber, W. A large-scale isolation of native β-lactoglobulin: characterization of physicochemical properties and comparison with other methods. *Int. Dairy J.* **2000**, *10* (10), 713–721.

(6) Gottschalk, M.; Nilsson, H.; Roos, H.; Halle, B. Protein self-association in solution: The bovine β-lactoglobulin dimer and octamer. *Protein Sci.* **2003**, *12* (11), 2404–2411.

(7) Chen, K.; Rana, S.; Moyano, D. F.; Xu, Y.; Guo, X.; Rotello, V. M. Optimizing the selective recognition of protein isoforms through tuning of nanoparticle hydrophobicity. *Nanoscale* **2014**, *6*, 6492–6495.

(8) Kurpiewska, K.; Biela, A.; Loch, J. I.; Świątek, S.; Jachimska, B.; Lewiński, K. Investigation of high pressure effect on the structure and adsorption of β-lactoglobulin. *Colloids Surfaces B Biointerfaces* **2018**, *161*, 387–393.

(9) Maity, S.; Pal, S.; Sardar, S.; Sepay, N.; Parvej, H.; Chakraborty, J.; Chandra Halder, U. Multispectroscopic analysis and molecular modeling to investigate the binding of beta-lactoglobulin with curcumin derivatives. *RSC Adv.* **2016**, *6* (113), 112175–112183.

(10) Domínguez-Ramírez, L.; Del Moral-Ramírez, E.; Cortes-Hernández, P.; Garibay, M. G.; Jiménez-Guzmán, J. β-lactoglobulin's conformational requirements for ligand binding at the calyx and the dimer interphase: A flexible docking study. *PLoS One* **2013**, *8* (11), 1–13.

(11) Hu, W.; Liu, J.; Luo, Q.; Han, Y.; Wu, K.; Lv, S.; Xiong, S.; Wang, F. Elucidation of the binding sites of sodium dodecyl sulfate to β-lactoglobulin using hydrogen/deuterium exchange mass spectrometry combined with docking simulation. *Rapid Commun. Mass Spectrom.* **2011**, *25* (10), 1429–1436.

(12) Yang, M. C.; Guan, H. H.; Liu, M. Y.; Lin, Y. H.; Yang, J. M.; Chen, W. L.; Chen, C. J.; Mao, S. J. T. Crystal structure of a secondary vitamin D3 binding site of milk β-lactoglobulin. *Proteins Struct. Funct. Genet.* **2008**, *71* (3), 1197–1210.

(13) Puyol, P.; Perez, M. D.; Ena, J. M.; Calvo, M. Interaction of bovine β-lactoglobulin and other bovine and human whey proteins with retinol and fatty acids. *Agric. Biol. Chem.* **1991**, *55* (10), 2515–2520.

(14) Wu, S. Y.; Pérez, M. D.; Puyol, P.; Sawyer, L. β-Lactoglobulin binds palmitate within its central cavity. *J. Biol. Chem.* **1999**, *274* (1), 170–174.

(15) Teng, Z.; Xu, R.; Wang, Q. Beta-lactoglobulin-based encapsulating systems as emerging bioavailability enhancers for nutraceuticals: a review. *RSC Adv.* **2015**, *5* (44), 35138–35154.

(16) Ohtomo, H.; Konuma, T.; Utsunoiya, H.; Tsuge, H.; Ikeguchi, M. Structure and stability of Gyuba, a β-lactoglobulin chimera. *Protein Sci.* **2011**, *20* (11), 1867–1875.

(17) Vijayalakshmi, L.; Krishna, R.; Sankaranarayanan, R.; Vijayan, M. An asymmetric dimer of β-lactoglobulin in a low humidity crystal form - Structural changes that accompany partial dehydration and protein action. *Proteins Struct. Funct. Genet.* **2008**, *71* (1), 241–249.

(18) Qin, B. Y.; Bewley, M. C.; Creamer, L. K.; Baker, H. M.; Baker, E. N.; Jameson, G. B. Structural basis of the tanford transition of bovine β-lactoglobulin. *Biochemistry* **1998**, *37* (40), 14014–14023.

(19) Qin, B. Y.; Creamer, L. K.; Baker, E. N.; Jameson, G. B. 12-Bromododecanoic acid binds inside the calyx of bovine β-lactoglobulin. *FEBS Lett.* **1998**, *438* (3), 272–278.

(20) Kuwata, K.; Hoshino, M.; Forge, V.; Era, S.; Batt, C. A.; Goto, Y. Solution structure and dynamics of bovine beta-lactoglobulin A. *Protein Sci.* **1999**, *8* (11), 2541–2545.

(21) Adams, J. J.; Anderson, B. F.; Norris, G. E.; Creamer, L. K.; Jameson, G. B. Structure of bovine β-lactoglobulin (variant A) at very low ionic strength. *J. Struct. Biol.* **2006**, *154* (3), 246–254.

(22) Guo, M.; Wang, G. Milk protein polymer and its application in environmentally safe adhesives. *Polymers (Basel). Polymers (Basel).* **2016**, *8* (9), 1–12.

(23) Moitzi, C.; Donato, L.; Schmitt, C.; Bovetto, L.; Gillies, G.; Stradner, A. Structure of β-lactoglobulin microgels formed during heating as revealed by small-angle X-ray scattering and light scattering. *Food Hydrocoll.* **2011**, *25* (7), 1766–1774.

(24) Sakurai, K.; Oobatake, M.; Goto, Y. Salt-dependent monomer – dimer equilibrium of bovine b-lactoglobulin at pH 3. *Protein Sci.* **2001**, *10*, 2325–2335.

(25) Baldini, G.; Beretta, S.; Chirico, G.; Franz, H.; Maccioni, E.; Mariani, P.; Spinozzi, F. Salt-induced association of β-lactoglobulin by light and X-ray scattering. *Macromolecules* **1999**, *32* (19), 6128–6138.

(26) Molinari, H.; Ragona, L.; Varani, L.; Musco, G.; Consonni, R.; Zetta, L.; Monaco, H. L. Partially folded structure of monomeric bovine β-lactoglobulin. *FEBS Lett.* **1996**, *381* (3), 237–243.

(27) Uhrínová, S.; Smith, M. H.; Jameson, G. B.; Uhrín, D.; Sawyer, L.; Barlow, P. N. Structural changes accompanying pH-induced dissociation of the β-lactoglobulin dimer. *Biochemistry* **2000**, *39* (13), 3565–3574.

(28) Oliveira, K. M.; Valente-Mesquita, V. L.; Botelho, M. M.; Sawyer, L.; Ferreira, S. T.; Polikarpov, I. Crystal structures of bovine β-lactoglobulin in the orthorhombic space group $C222_1$. *Eur. J. Biochem.* **2001**, *268* (2), 477–484.

(29) Qin, B. Y.; Bewley, M. C.; Creamer, L. K.; Baker, E. N.; Jameson, G. B. Functional implications of structural differences between variants A and B of bovine β-lactoglobulin. *Protein Sci.* **1999**, *8* (1), 75–83.

(30) Madureira, A. R.; Pereira, C. I.; Gomes, A. M. P.; Pintado, M. E.; Xavier Malcata, F. Bovine whey proteins - overview on their main biological properties. *Food Res. Int.* **2007**, *40* (10), 1197–1211.

(31) Townend, R.; Timasheff, S. N. Molecular interactions in β-lactoglobulin. III. Light scattering investigation of the stoichiometry of the association between pH 3.7 and 5.2. *J. Am. Chem. Soc.* **1960**, *82* (12), 3168–3174.

(32) Kumosinski, T. F.; Timasheff, S. N. *J.* Molecular interactions in β-lactoglobulin. X. The stoichiometry of the β-lactoglobulin mixed tetramerization. *Am. Chem. Soc.* **1966**, *88* (23), 5635–5642.

(33) Verheul, M.; Pedersen, J. S.; Roefs, S. P. F. M.; de Kruif, K. G. Association behavior of native β-lactoglobulin. Biopolymers, **1999**, *49*, 11–20.

(34) Mercadante, D.; Melton, L. D.; Norris, G. E.; Loo, T. S.; Williams, M. A. K.; Dobson, R. C. J.; Jameson, G. B. Bovine β-lactoglobulin is dimeric under imitative physiological conditions: Dissociation equilibrium and rate constants over the pH range of 2.5–7.5. *Biophys. J.* **2012**, *103* (2), 303–312.

(35) Kristiansen, K. R.; Otte, J.; Ipsen, R.; Qvist, K. B. Large-scale preparation of β-lactoglobulin A and B by ultrafiltration and ion-exchange chromatography. *Int. Dairy J.* **1998**, *8* (2), 113–118.

(36) Collini, M.; D'Alfonso, L.; Baldini, G. New insight on β-lactoglobulin binding sites by 1-anilinonaphthalene-8-sulfonate fluorescence decay. *Protein Sci*. **2000**, *9* (10), 1968–1974.

(37) Kabsch, W. *J.* Automatic processing of rotation diffraction data from crystals of initially unknown symmetry and cell constants. *Appl. Cryst*. **1993**. *26*, 795–800.

(38) McCoy, A. J.; Grosse-Kunstleve, R. W.; Adams, P. D.; Winn, M. D.; Storoni, L. C.; Read, R. J. Phaser crystallographic software. *J. Appl. Crystallogr.* **2007**, *40* (4), 658–674.

(39) Afonine, P. V.; Grosse-Kunstleve, R. W.; Echols, N.; Headd, J. J.; Moriarty, N. W.; Mustyakimov, M.; Terwilliger, T. C.; Urzhumtsev, A.; Zwart, P. H.; Adams, P. D. Towards automated crystallographic structure refinement with phenix.refine. *Acta Crystallogr. Sect. D Biol. Crystallogr.* **2012**, *68* (4), 352–367.

(40) Emsley, P.; Cowtan, K. Coot: model-building tools for molecular graphics. *Acta Crystallogr. Sect. D Biol. Crystallogr.* **2004**, *60* (12 I), 2126–2132.

(41) Zwart, P. H.; Afonine, P. V; Grosse-kunstleve, R. W.; Hung, L.; Ioerger, T. R.; Mccoy, A. J.; Mckee, E.; Moriarty, N. W.; Read, R. J.; Sacchettini, J. C.; Sauter, N. K.; Storoni, L. C.; Terwilliger, T. C.; Adams, P. D. Automated structure solution with the PHENIX suite. *Methods Mol. Biol.* **2008**, *426*, 419–435.

(42) Adams, P. D.; Afonine, P. V.; Bunkóczi, G.; Chen, V. B.; Davis, I. W.; Echols, N.; Headd, J. J.; Hung, L. W.; Kapral, G. J.; Grosse-Kunstleve, R. W.; McCoy, A. J.; Moriarty, N. W.; Oeffner, R.; Read, R. J.; Richardson, D. C.; Richardson, J. S.; Terwilliger, T. C.; Zwart, P. H. PHENIX: A comprehensive Python-based system for macromolecular structure solution. *Acta Crystallogr. Sect. D Biol. Crystallogr.* **2010**, *66* (2), 213–221.

(43) Narayanan, T.; Diat, O.; Bösecke, P. SAXS and USAXS on the high brilliance beamline at the ESRF. *Nucl. Instruments Methods Phys. Res. Sect. A Accel. Spectrometers, Detect. Assoc. Equip.* **2001**, *467–468* (PART II), 1005–1009.

(44) Blanchet, C. E.; Spilotros, A.; Schwemmer, F.; Graewert, M. A.; Kikhney, A.; Jeffries, C. M.; Franke, D.; Mark, D.; Zengerle, R.; Cipriani, F.; Fiedler, S.; Roessle, M.; Svergun, D. I. Versatile sample environments and automation for biological solution X-ray scattering experiments at the P12 beamline (PETRA III, DESY). *J. Appl. Crystallogr.* **2015**, *48*, 431–443.

(45) Petoukhov, M. V.; Franke, D.; Shkumatov, A. V.; Tria, G.; Kikhney, A. G.; Gajda, M.; Gorba, C.; Mertens, H. D. T.; Konarev, P. V.; Svergun, D. I. New developments in the ATSAS program package for small-angle scattering data analysis. *J. Appl. Crystallogr.* **2012**, *45* (2), 342–350.

(46) Svergun, D. I. Determination of the regularization parameter in indirect-transform methods using perceptual criteria. *J. Appl. Crystallogr.* **1992**, *25* (pt 4), 495–503.

(47) Okemefuna, A. I.; Nan, R.; Gor, J.; Perkins, S. J. Electrostatic interactions contribute to the folded-back conformation of wild type human factor H. *J. Mol. Biol.* **2009**, *391* (1), 98–118.

(48) Wright, D. W.; Perkins, S. J. SCT: a suite of programs for comparing atomistic models with small-angle scattering data. *J. Appl. Crystallogr.* **2015**, *48* (Pt 3), 953–961.

(49) Ashton, A. W.; Boehm, M. K.; Gallimore, J. R.; Pepys, M. B.; Perkins, S. J. Pentameric and decameric structures in solution of serum amyloid P component by X-ray and neutron scattering and molecular modelling analyses. *J. Mol. Biol.* **1997**, *272* (3), 408–422.

(50) Khan, S.; Birch, J.; Harris, P.; Van Calsteren, M.-R.; Ipsen, R.; Peters, G. H. J.; Svensson, B.; Almdal, K. Revealing the compact structure of lactic acid bacterial heteroexopolysaccharides by SAXS and DLS. *Biomacromolecules* **2017**, *18* (3), 747–756.

(51) The PyMOL molecular graphics system, version 1.3.Schrödinger, LLC; New York, NY:

(52) Loch, J. I.; Bonarek, P.; Tworzydło, M.; Polit, A.; Hawro, B.; Łach, A.; Ludwin, E.; Lewiński, K. Engineered β-lactoglobulin produced in *E. coli*: purification, biophysical and structural characterisation. *Mol. Biotechnol*. **2016**, *58* (10), 605–618.

(53) Townend, R.; Weinberger, L.; Timasheff, S. N. Molecular interactions in βlactoglobulin. IV. The dissociation of β-lactoglobulin below pH 3.5. *J. Am. Chem. Soc*. **1960**, *82*, 3175–3179.

(54) Townend, R.; Kiddy, C. A.l; Timasheff, S. N. Molecular interactions in βlactoglobulin. VII. The hybridization of β-lactoglobulins A and B. *J. Am. Chem. Soc*. **1961**, *83*, 1419–1423.

(55) Bello, M.; Perez-Hernandez G.; Fernandez-Velasco, D. A.; Arreguin-Espinosa, R.; Garcia-Hernandez E. Energetics of protein homodimerization: effects of water sequestering on the formation of β-lactoglobulin dimer. *Proteins*: *Struct. Funct. Bioinf*. 2008, *70*, 1475–1487.

(56) Kelly, M. J.; Reithel. F. J. Thermodynamic analysis of the monomer-dimer association of β-lactoglobulin A at the isoelectric point. Biochemistry 1971, *10*, 2639–2644.

(57) Zimmerman, J. K.; Barlow, G. H.; Klotz, I. M. Dissociation of βlactoglobulin near neutral pH. *Arch. Biochem. Biophys*. **1970**. *138*, 101-109.

(58) Teng, Z.; Li, Y.; Luo, Y.; Zhang, B.; Wang, Q. Cationic β-lactoglobulin nanoparticles as a bioavailability enhancer: protein characterization and particle formation. *Biomacromolecules* **2013**, *14*, 2848–2856.

(59) Teng, Z.; Luo, Y.; Li, Y.; Wang, Q. Cationic β-lactoglobulin nanoparticles as a bioavailability enhancer: Effect of surface properties and size on the transport and delivery in vitro. *Food Chem.* **2016**, *204*, 391–399.

(60) Izadi, Z.; Divsalar, A.; Saboury, A. A.; Sawyer, L. β-lactoglobulin–pectin nanoparticle-based oral drug delivery system for potential treatment of colon cancer. *Chem. Biol. Drug Des.* **2016**, *88* (2), 209–216.

(61) Jones, O. G.; Lesmes, U.; Dubin, P.; McClements, D. J. Effect of polysaccharide charge on formation and properties of biopolymer nanoparticles created by heat treatment of β-lactoglobulin-pectin complexes. *Food Hydrocoll.* **2010**, *24* (4), 374–383.

(62) McAlpine, A. S.; Sawyer, L. β-lactoglobulin: a protein drug carrier? *Biochem. Soc. Trans.* **1990**, *18* (5), 879.

(63) Harnsilawat, T.; Pongsawatmanit, R.; McClements, D. J. Characterization of β-lactoglobulin-sodium alginate interactions in aqueous solutions: A calorimetry, light scattering, electrophoretic mobility and solubility study. *Food Hydrocoll.* **2006**, *20* (5), 577–585.

TOC

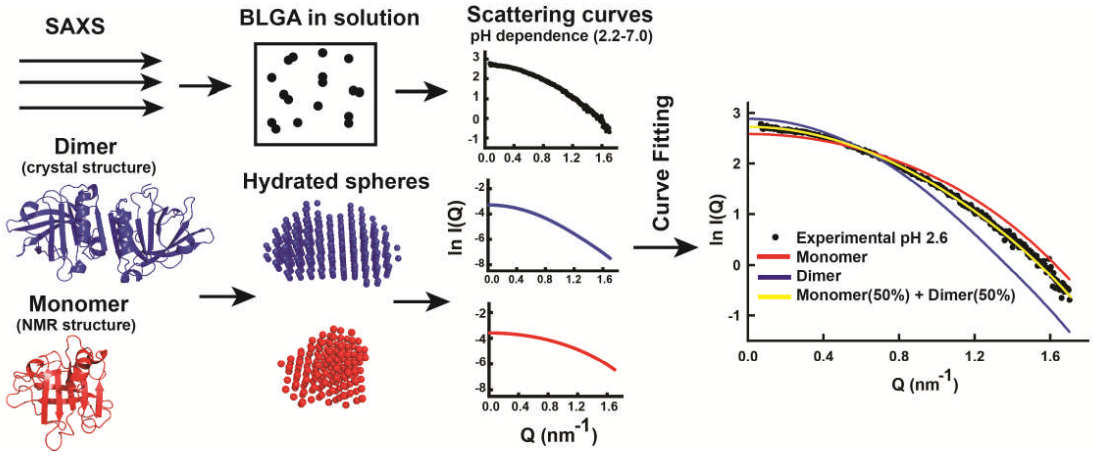
SAXS
BLGA in solution
Scattering curves
pH dependence (2.2-7.0)
Dimer
(crystal structure)
Hydrated spheres
Monomer
(NMR structure)
ln I(Q)
Q (nm-1)
Curve Fitting
Experimental pH 2.6
Monomer
Dimer
Monomer(50%) + Dimer(50%)